Aggregation properties of a short peptide that mediates amyloid fibril formation in model proteins unrelated to disease

NITIN CHAUDHARY, SHASHI SINGH and RAMAKRISHNAN NAGARAJ*
Centre for Cellular and Molecular Biology, Uppal Road, Hyderabad 500 007
India
**Corresponding author (Fax, +91-40-27160591/27160311; Email, nraj@ccmb.res.in)*

Recto running title: *Aggregation properties of a short peptide*
Verso running title: *N Chaudhary, S Singh and R Nagaraj*

Abstract

Short peptides have been identified from amyloidogenic proteins that form amyloid fibrils in isolation. The hexapeptide stretch ^{21}DIDLHL^{26} has been shown to be important in the self-assembly of the Src homology 3 (SH3) domain of p85α subunit of bovine phosphatidylinositol-3-kinase (PI3-SH3). The SH3 domain of chicken brain α-spectrin, which is otherwise non-amyloidogenic, is rendered amyloidogenic if ^{22}EVTMKK^{27} is replaced by DIDLHL. In this article, we describe the aggregation behaviour of DIDLHL-COOH and DIDLHL-$CONH_2$. Our results indicate that DIDLHL-COOH and DIDLHL-$CONH_2$ aggregate to form spherical structures at pH 5 and 6. At pH 5, in the presence of mica, DIDLHL-$CONH_2$ forms short fibrous structures. The presence of NaCl along with mica results in fibrillar structures. At pH 6, DIDLHL-$CONH_2$ forms largely spherical aggregates. Both the peptides are unstructured in solution but adopt β-conformation on drying. The aggregates formed by DIDLHL-COOH and DIDLHL-$CONH_2$ are formed during drying process and their structures are modulated by the presence of mica and salt. Our study suggests that a peptide need not have intrinsic amyloidogenic propensity to facilitate the self-assembly of the full-length protein. The propensity of peptides to form self-assembled structures that are non-amyloidogenic could be important in potentiating the self-assembly of full-length proteins into amyloid fibrils.

[Chaudhary N, Singh S and Nagaraj R 2011 Aggregation properties of a short peptide that mediates amyloid fibril formation in model proteins unrelated to disease. *J. Biosci.* **36** XXX–XXX] **DOI**

Keywords. Amyloid fibrils; atomic force microscopy; non-fibrillar structures; peptide self-association; SH3 domain

Abbreviations used: AFM, atomic force microscopy; ATR, attenuated total reflection; CD, circular dichroism; D-ac, NH_2–DIDLHL–COOH; D-am, NH_2–DIDLHL–$CONH_2$; FTIR, Fourier transform infrared spectra; MALDI-TOF, matrix-assisted laser desorption ionization-time-of-flight; PI3-SH3, phosphatidylinositol-3-kinase; SH3, Src homology 3; SPC-SH3, SH3 domain of chicken brain α-spectrin; TFA, trifluoroacetic acid

1. Introduction

Peptides with highly variable lengths and amino acid sequences have been observed to form amyloid fibrils (Jarvis *et al.* 1993; Tenidis *et al.* 2000; Lopez De La Paz *et al.* 2002; Reches *et al.* 2002; Tjernberg *et al.* 2002; Jones *et al.* 2003; Goux *et al.* 2004). While many of these peptides are segments of proteins that form fibrils *in vivo* and are related to pathogenesis (Jarvis

et al. 1993; Tenidis *et al.* 2000; Reches *et al.* 2002; Goux *et al.* 2004), others are unrelated to pathogenesis (Fezoui *et al.* 2000; Lopez De La Paz *et al.* 2002; Tjernberg *et al.* 2002). The conditions under which peptides form fibrils vary considerably with respect to pH, ionic strength, temperature, aggregation times as well as the presence of organic solvents (Burdick *et al.* 1992; Harper *et al.* 1999; Thompson *et al.* 2000; Goux *et al.* 2004; Chaudhary *et al.* 2008; Chaudhary *et al.* 2009). Amyloid formation by peptides and proteins has also been observed on solid substrates such as mica or quartz (Zhu *et al.* 2002; Losic *et al.* 2006).

The amyloid forming ability of peptides that are segments of amyloid-forming proteins has been the subject of extensive investigation (Tenidis *et al.* 2000; Kozhukh *et al.* 2002; Reches *et al.* 2002; Jones *et al.* 2003; Goux *et al.* 2004; Ivanova *et al.* 2006; Thompson *et al.* 2006). It appears that the peptide segments, in isolation, do have the ability to form fibrils that are very similar to the fibrils formed by the parent proteins. These peptide fibrils have the conformational features of β-structure that are observed in protein fibrils (Giasson *et al.* 2001; Iconomidou *et al.* 2001; Iconomidou *et al.* 2000; Fandrich *et al.* 2003; Jones *et al.* 2003).

The Src homology 3 (SH3) domain of p85α subunit of bovine phosphatidylinositol-3-kinase (PI3-SH3) forms amyloid fibrils at acidic pH (pH 2.0), while the SH3 domain of chicken brain α-spectrin (SPC-SH3), which shares same fold and 24% sequence identity with PI3-SH3, does not form fibrils under these conditions (Guijarro *et al.* 1998; Ventura *et al.* 2004). At pH 2.0, the PI3-SH3 domain is partially denatured following which the domain self-assembles into amyloid-like fibrils. The presence of extensive native-like interactions in SPC-SH3 under acidic pH, as suggested by solution NMR studies (Kortemme *et al.* 2000), may account for its inability to form amyloid fibrils under these conditions. Replacing a six-amino-acid stretch (^{22}EVTMKK^{27}) in SPC-SH3 with PI3-SH3 hexapeptide ^{21}DIDLHL^{26}, comprising residues in the diverging turn and adjacent RT loop, confers amyloidogenicity to SPC-SH3 (Ventura *et al.* 2004). Replacement of residues HL in the DIDLHL segment of PI3-SH3 by consensus residues KK renders the domain non-amyloidogenic, indicating the importance of the DIDLHL sequence in conferring amyloidogenicity to the domain. Interestingly, both amyloidogenic and non-amyloidogenic forms of PI3-SH3 are denatured to similar extent at pH 2.0 (Ventura *et al.* 2004). This suggests that the sequence DIDLHL does not affect the stability of SH3 domain in conferring amyloidogenicity to it. In this study, we have investigated the aggregation behavior of NH_2–DIDLHL–$CONH_2$ (D-am) and NH_2–DIDLHL–COOH (D-ac) under various conditions.

2. Materials and methods

Fmoc amino acids were purchased from Novabiochem AG (Switzerland) and Advanced ChemTech (Louisville, KY). Peptide synthesis resins, HMP (p-Hydroxymethylphenoxymethyl polystyrene resin) and PAL (5-(4-Aminomethyl-3,5-dimethoxyphenoxy)valeric acid resin) were purchased from Applied Biosystems (Foster City, CA) and Advanced ChemTech (Louisville, KY), respectively. Thioflavin T was purchased from Sigma.

2.1 *Peptide synthesis*

The peptides NH_2–DIDLHL–$CONH_2$ (D-am) and NH_2–DIDLHL–COOH (D-ac) were synthesized using standard Fmoc chemistry (Atherton 1989). The synthesized peptides were cleaved from the resin and deprotected using a mixture containing 82.5% trifluoroacetic acid (TFA), 5% phenol, 5% H_2O, 5% thioanisole and 2.5% ethanedithiol for 12–15 h at room temperature (King *et al.* 1990). The peptides were precipitated in ice-cold diethyl ether. The peptides were dissolved in deionized water and purified on Hewlett Packard 1100 series HPLC instrument on a reversed-phase C18 Bio-Rad column using a linear gradient of H_2O-acetonitrile,

both containing v/v 0.1% TFA. Purified peptides were characterized using matrix-assisted laser desorption ionization-time-of-flight (MALDI-TOF) mass spectrometry on a Voyager DE STR mass spectrometer (PerSeptive Biosystems, Foster city, CA) in the Proteomics Facility at the Centre for Cellular and Molecular Biology, India. The spectra of the peptides showed *m*/*z* values of 724.26 for D-am (calculated mass: 723.80 Da) and 725.24 for D-ac (calculated mass: 724.80 Da). Stock solutions of the peptides were prepared in deionized water and concentrations were determined using Waddell's method of protein concentration estimation (Waddell 1956; Wolf 1983).

2.2 *Aggregation reactions*

Aggregation reactions at 200 μM peptide concentration were set up for both D-am and D-ac in 10 mM acetate buffer, pH 5, and 10 mM phosphate buffer, pH 6, with/without 100 mM NaCl and with/without freshly cleaved mica piece at 37°C for 5 days. These pH values were chosen for the studies after screening the pH range of 2–12 for aggregation. Samples having mica were prepared as follows: after preparing the peptide solution in the desired buffer, a rectangular piece of mica was immediately dropped into the sample tube. Both the surfaces of the mica piece were freshly peeled prior to dropping it in the sample tube. Aggregation of all the samples was studied using atomic force microscopy.

2.3 *Atomic force microscopy*

Aggregation reaction samples were diluted in deionized water and immediately deposited on freshly cleaved surface of mica sheets (≤1 μg peptide was deposited) and allowed to dry in air. Atomic force microscopy (AFM) images were acquired in an atomic force microscope (Multimode, Digital Instruments, Santa Barbara, CA) using tapping mode. A silicon nitride probe was oscillated at 275–310 kHz and images were collected at an optimized scan rate. Analysis was done using Nanoscope ® III 5.30 r1. All the images are second order flattened and presented in the height mode. Height analysis was done using 'Section' tool present in the Nanoscope software. 512×512 points were acquired for each AFM image. The individual images were re-sized to obtain the desired resolution of 300 dots per inch.

2.4 *Circular dichroism*

Circular dichroism (CD) spectra were recorded on Jasco J-715 spectropolarimeter. Far-UV spectra (195–250 nm) were recorded for 120 μM peptide solutions in 10 mM actetate buffer, pH 5, and 10 mM phosphate buffer, pH 6, with/without 100 mM NaCl in 0.1 cm path length cell using a step size of 0.2 nm, band width of 1 nm, and scan rate of 100 nm/min. The spectra were recorded by averaging eight scans and corrected by subtracting the buffer spectra.

2.5 *Fourier transform infrared spectroscopy*

Fourier transform infrared spectra (FTIR) were recorded on a Bruker Alpha-E spectrometer with Eco attenuated total reflection (ATR) single reflection ATR sampling module equipped with ZnSe ATR crystal. Peptide solutions (200 μM) were prepared in deionized water without exchanging TFA counterions. Peptide solutions (20 μl) were spread out and dried as films on ZnSe crystal and ATR-FTIR spectra were recorded. Each spectrum is the average of 64 FTIR spectra at a resolution of 4 cm^{-1}.

3. Results and discussion

The peptide segment DIDLHL has been shown to promote the formation of amyloid fibrils in PI3-SH3 and α-spectrin-SH3 domains (Guijarro *et al.* 1998; Ventura *et al.* 2004). Two peptides, D-ac and D-am, were examined for their ability to form aggregates under different

conditions such as pH, salt concentration and the presence of mica. The aggregates were characterized by AFM. Along with the AFM images, a height profile of a line segment drawn on the figure is also shown. The height of one aggregate in each AFM figure has been indicated with black triangle.

The aggregates of D-ac at pH 5 and 6, in the presence of salt and mica, were examined (figure 1). At pH 6, largely spherical aggregates (heights ~1–6 nm) are observed (figure 1A and B). A few linear fibrils (~2–3 nm thick, indicated by arrows) associated with spherical aggregates are also observed. The heights of the fibrils are indicated by black triangles. In the presence of mica, at pH 6, only spherical aggregates (~2–12 nm) are observed (figure 1C). At pH 5, too, in the presence of 100 mM NaCl, only spherical aggregates (~2–10 nm) are observed (figure 1D). The presence of mica does not cause any significant change in the aggregates (data not shown).

The aggregates formed by D-am under different conditions were examined. At pH 5, D-am forms spherical aggregates up to 35 nm in diameter (figure 2). An aggregate ~23 nm in height is labelled with the black triangle. The dragging of the aggregates towards right could arise from tip-sample interactions. In the presence of mica at pH 5, small fibrillar aggregates are observed (figure 3). Figure 3A shows presence of small fibrous structures (2–6 nm in thickness). In figure 3B, a mixture of very small aggregates, thin fibrils (<1–3 nm) and thicker fibrillar structures (3–6 nm, indicated by arrows) are observed. When NaCl is also present along with mica, fibrillar aggregates are observed (figure 4). The panels show images recorded from 4 independently prepared samples. The fibrils show considerable polymorphism. The dimensions of the fibrils vary considerably (thickness ranging from 1–10 nm). Figure 4A–C shows fibers that appear similar to amyloid protofibrils in dimensions (heights ≤3.5 nm, lengths <1 μm). The fibrils in figure 4D vary in diameter from very thin to those typical of amyloid protofilaments and amyloid fibrils (~1–10 nm).

The D-am aggregates obtained at pH 6 are shown in figure 5. The panels represent independent samples. Fibril formation was no longer discernible. Individual spheres, very small to very large (~3–50 nm) are observed (figure 5A and B). In one case, large oval egg-shaped structures (figure 5C) were observed. Even in the presence of either mica (figure 6A) or NaCl (figure 6B) during aggregation process, mostly spherical aggregates are observed with very few thin filamentous structures figure 6A). While aggregates with different morphologies were detected for D-am and D-ac by AFM, none of them caused any increase in Thioflavin T fluorescence (data not shown), indicating that the peptide sequences do not form mature amyloid fibrils under the conditions studied.

Amide I region in FTIR spectra is sensitive to secondary structures of proteins and peptides as it largely arises from C=O stretching vibrations with a small contribution from NH bending (Surewicz *et al.* 1993; Haris and Chapman 1995; Jackson and Mantsch 1995). The peptides were dried on ZnSe crystal from water and attenuated total reflectance-FTIR (ATR-FTIR) spectra were recorded on dry peptide films to correlate the peptide secondary structures with self-assembled structures on mica (figure 7). Amide I absorption band centered at 1631 cm^{-1} was observed for D-am (figure 7A), while D-ac amide I band was centered at 1637 cm^{-1} (figure 7B). The amide I frequencies from 1625 to 1640 cm^{-1} correspond to β-sheet structure, while 1640–1648 cm^{-1} corresponds to unordered polypeptide chain (Jackson and Mantsch 1995). The data suggest that both D-am and D-ac adopt β-structure in the dried form. However, the amide I band of D-ac at 1637 cm^{-1} indicates more unordered component as compared with that

in D-am, which correlates with its lower propensity to form fibrillar structures. In solution, secondary structures at pH 5 and 6 with/without 100 mM NaCl were studied using CD spectroscopy. CD spectra of both the peptides are suggestive of unordered conformation irrespective of the presence or absence of NaCl (figure 8). These results clearly suggest that the peptides self-assemble by adopting β-conformation during drying process.

In vitro, proteins that form fibrils under disease conditions, as well as peptides with widely differing sequences, form fibrils and other aggregated structures that exhibit highly variable morphologies (Bauer *et al.* 1995; Kad *et al.* 2001; Lopez De La Paz *et al.* 2002; Goux *et al.* 2004; Goldsbury *et al.* 2005; Kardos *et al.* 2005; Petkova *et al.* 2005; Anderson *et al.* 2006; Paravastu *et al.* 2006). Even fibrils produced under single growth conditions display considerable variation in their morphologies from the same sample preparation (Jansen *et al.* 2005; Anderson *et al.* 2006). In the case of insulin and Aβ, spherical structures appear to precede fibril formation (Blackley *et al.* 2000; Goldsbury *et al.* 2005; Jansen *et al.* 2005). Thus, the process of mature fibril formation appears to proceed via several intermediate aggregates, which are not necessarily fibrillar. In fact, the initial structure need not even be a β-structure (Fezoui *et al.* 2000; Fandrich *et al.* 2001; von Bergen *et al.* 2005). A highly amyloidogenic peptide derived from the Aβ sequence has a polyproline II like structure (Gnanakaran *et al.* 2006). Short peptides, which are unlikely to adopt ordered secondary structure, have been shown to self-assemble into ordered aggregates (Gorbitz 2001; Reches and Gazit 2003; Reches and Gazit 2006). The peptide, Ac-VYK-am, adopts random coil conformation as suggested by CD, and does not cause enhancement in ThT fluorescence (Goux *et al.* 2004). However, the peptide forms fibrillar aggregates as observed using electron microscopy (Goux *et al.* 2004). We find that fibrils were observed for D-am but not for D-ac. Fibrils were observed at pH 5 and non-fibrillar oligomeric structures were observed at pH 6. The pK_{a2} of histidine is 6.0. At pH 5, ~90% of the histidine would be positively charged. Therefore, D-ac would have a net charge of −1, while D-am would have net charge of 0. It appears that net charge on the peptide influences its self-association. Mica, which has a negatively charged surface, could interact with the peptide via electrostatic interactions. NaCl would shield any charge present on the peptide further driving its self-association, probably through stabilization of hydrophobic interactions.

Our results with DIDLHL peptides indicate their propensities to form spherical aggregates as well as filamentous structures. However, we have not been able to observe the transformation of these soluble aggregates into insoluble amyloid fibril structures. Under the conditions of low pH, at which PI3-SH3 forms fibrils, the DIDLHL sequence might act as a facilitator that promotes the formation of fibrils with other regions of the protein, probably through charge compensation and hydrophobic interactions (von Bergen *et al.* 2001; Chiba *et al.* 2003). Distal peptide sequences have been shown to facilitate amyloid formation in proteins such as β_2-microglobulin (Ivanova *et al.* 2004). The ability to potentiate the formation of aggregates could be the reason for the induction of aggregation by DIDLHL in α-spectrin-SH3 domain, which, on its own, does not form fibrils (Kortemme *et al.* 2000). It has been observed that a single mutation can cause α-spectrin-SH3 domain to form fibrillar aggregates indicating that the protein could be prone to destabilization resulting in fibril formation (Morel *et al.* 2006). However, replacement of ^{25}HL^{26} in PI3-SH3 with the consensus KK sequence does not affect its stability but renders it non-amyloidogenic. This suggests that the sequence, DIDLHL may not be required for the stability of the SH3 domain but is important for conferring amyloidogenicity to

it, further suggesting that the stretch might act as a facilitator in amyloid formation by interacting with other aggregation-prone stretches present in the domain.

4. Conclusions

Our results with DIDLHL peptides indicate their ability to form spherical aggregates as well as filamentous structures. However, we have not been able to observe the formation of amyloid fibril structures. Although fibrillar structures were obtained for D-am at pH 5 in the presence of salt and mica, their amyloid nature is not confirmed. Amyloid fibrils cause enhancement in ThT fluorescence and their amide I band in FTIR spectra appear at ~1620–1629 cm^{-1} (Tracz *et al.* 2004; Yamaguchi *et al.* 2005). Absence of these features suggests that the fibrils formed by D-am may not be classical amyloid-like. Formation of fibrils by only certain short peptide segments of amyloid forming proteins suggests an important role for such sequences in the formation of fibrils by the mature protein (Giasson *et al.* 2001; Kozhukh *et al.* 2002; Jones *et al.* 2003). In several cases, changes in the sequence of these peptides abrogate fibril formation suggesting that the requirement may be stringent (von Bergen *et al.* 2000). Our results with DIDLHL suggest that it may not be necessary in all the cases for the peptide, presumed to play a role in amyloid formation, to form mature fibrils in isolation. The ability to aggregate, particularly to form aggregates of various morphologies, could be sufficient to induce fibril formation in the protein. *In vivo*, peptides and proteins are likely to encounter surfaces and interfaces which could modulate amyloid fibril formation as demonstrated for Aβ (Losic *et al.* 2006) and recombinant amyloidogenic light chain variable domain (Zhu *et al.* 2002). Hence, self-assembly of peptides related to the process of amyloid formation at surfaces or interfaces could have physiological relevance.

Acknowledgements

This work was funded by CSIR under the Network Project NWP035.

References

Anderson M, Bocharova OV, Makarava N, Breydo L, Salnikov VV and Baskakov IV 2006 Polymorphism and ultrastructural organization of prion protein amyloid fibrils: an insight from high resolution atomic force microscopy. *J. Mol. Biol.* **358** 580–596

Atherton E 1989 *Solid phase synthesis: A practical approach* (Oxford: IRL Press)

Bauer HH, Aebi U, Haner M, Hermann R, Muller M and Merkle HP 1995 Architecture and polymorphism of fibrillar supramolecular assemblies produced by in vitro aggregation of human calcitonin. *J Struct Biol* 115 1–15

Blackley HK, Sanders GH, Davies MC, Roberts CJ, Tendler SJ and Wilkinson MJ 2000 In-situ atomic force microscopy study of beta-amyloid fibrillization. *J. Mol. Biol.* **298** 833–840

Burdick D, Soreghan B, Kwon M, Kosmoski J, Knauer M, Henschen A, Yates J, Cotman C, *et al.* 1992 Assembly and aggregation properties of synthetic Alzheimer's A4/beta amyloid peptide analogs. *J. Biol. Chem.* **267** 546–554

Chaudhary N, Singh S and Nagaraj R 2008 Organic solvent mediated self-association of an amyloid forming peptide from beta2-microglobulin: an atomic force microscopy study. *Biopolymers* **90** 783–791

Chaudhary N, Singh S and Nagaraj R 2009 Morphology of self-assembled structures formed by short peptides from the amyloidogenic protein tau depends on the solvent in which the peptides are dissolved. *J. Pept. Sci.* **15** 675–684

Chiba T, Hagihara Y, Higurashi T, Hasegawa K, Naiki H and Goto Y 2003 Amyloid fibril formation in the context of full-length protein: effects of proline mutations on the amyloid fibril formation of beta2-microglobulin. *J. Biol. Chem.* **278** 47016–47024

Fandrich M, Fletcher MA and Dobson CM 2001 Amyloid fibrils from muscle myoglobin. *Nature (London)* **410** 165–166

Fandrich M, Forge V, Buder K, Kittler M, Dobson CM and Diekmann S 2003 Myoglobin forms amyloid fibrils by association of unfolded polypeptide segments. *Proc. Natl. Acad. Sci. USA* **100** 15463–15468

Fezoui Y, Hartley DM, Walsh DM, Selkoe DJ, Osterhout JJ and Teplow DB 2000 A de novo designed helix-turn-helix peptide forms nontoxic amyloid fibrils. *Nat. Struct. Biol.* **7** 1095–1099

Giasson BI, Murray IV, Trojanowski JQ and Lee VM 2001 A hydrophobic stretch of 12 amino acid residues in the middle of alpha-synuclein is essential for filament assembly. *J. Biol. Chem.* **276** 2380–2386

Gnanakaran S, Nussinov R and Garcia AE 2006 Atomic-level description of amyloid beta-dimer formation. *J. Am. Chem. Soc.* **128** 2158–2159

Goldsbury C, Frey P, Olivieri V, Aebi U and Muller SA 2005 Multiple assembly pathways underlie amyloid-beta fibril polymorphisms. *J. Mol. Biol.* **352** 282–298

Gorbitz CH 2001 Nanotube formation by hydrophobic dipeptides. *Chemistry – Eur. J.* **7** 5153–5159

Goux WJ, Kopplin L, Nguyen AD, Leak K, Rutkofsky M, Shanmuganandam VD, Sharma D, Inouye H, *et al.* 2004 The formation of straight and twisted filaments from short tau peptides. *J. Biol. Chem.* **279** 26868–26875

Guijarro JI, Sunde M, Jones JA, Campbell ID and Dobson CM 1998 Amyloid fibril formation by an SH3 domain. *Proc. Natl. Acad. Sci. USA* **95** 4224–4228

Haris PI and Chapman D 1995 The conformational analysis of peptides using Fourier transform IR spectroscopy. *Biopolymers* **37** 251–263

Harper JD, Wong SS, Lieber CM and Lansbury PT Jr 1999 Assembly of A beta amyloid protofibrils: an in vitro model for a possible early event in Alzheimer's disease. *Biochemistry* **38** 8972–8980

Iconomidou VA, Chryssikos GD, Gionis V, Vriend G, Hoenger A and Hamodrakas SJ 2001 Amyloid-like fibrils from an 18-residue peptide analogue of a part of the central domain of the B-family of silkmoth chorion proteins. *FEBS Lett.* **499** 268–273

Iconomidou VA, Vriend G and Hamodrakas SJ 2000 Amyloids protect the silkmoth oocyte and embryo. *FEBS Lett.* **479** 141–145

Ivanova MI, Sawaya MR, Gingery M, Attinger A and Eisenberg D 2004 An amyloid-forming segment of beta2-microglobulin suggests a molecular model for the fibril. *Proc. Natl. Acad. Sci. USA* **101** 10584–10589

Ivanova MI, Thompson MJ and Eisenberg D 2006 A systematic screen of beta(2)-microglobulin and insulin for amyloid-like segments. *Proc. Natl. Acad. Sci. USA* **103** 4079–4082

Jackson M and Mantsch HH 1995 The use and misuse of FTIR spectroscopy in the determination of protein structure. *Crit. Rev. Biochem. Mol. Biol.* **30** 95–120

Jansen R, Dzwolak W and Winter R 2005 Amyloidogenic self-assembly of insulin aggregates probed by high resolution atomic force microscopy. *Biophys. J.* **88** 1344–1353

Jarvis JA, Craik DJ and Wilce MC 1993 X-ray diffraction studies of fibrils formed from peptide fragments of transthyretin. *Biochem. Biophys. Res. Commun.* **192** 991–998

Jones S, Manning J, Kad NM and Radford SE 2003 Amyloid-forming peptides from beta2-microglobulin-Insights into the mechanism of fibril formation in vitro. *J. Mol. Biol.* **325** 249–257

Kad NM, Thomson NH, Smith DP, Smith DA and Radford SE 2001 Beta(2)-microglobulin and its deamidated variant, N17D form amyloid fibrils with a range of morphologies in vitro. *J. Mol. Biol.* **313** 559–571

Kardos J, Okuno D, Kawai T, Hagihara Y, Yumoto N, Kitagawa T, Zavodszky P, Naiki H *et al.* 2005 Structural studies reveal that the diverse morphology of beta(2)-microglobulin aggregates is a reflection of different molecular architectures. *Biochim. Biophys. Acta* **1753** 108–120

King DS, Fields CG and Fields GB 1990 A cleavage method which minimizes side reactions following Fmoc solid phase peptide synthesis. *Int. J. Pept. Protein Res.* **36** 255–266

Kortemme T, Kelly MJ, Kay LE, Forman-Kay J and Serrano L 2000 Similarities between the spectrin SH3 domain denatured state and its folding transition state. *J. Mol. Biol.* **297** 1217–1229

Kozhukh GV, Hagihara Y, Kawakami T, Hasegawa K, Naiki H and Goto Y 2002 Investigation of a peptide responsible for amyloid fibril formation of beta 2-microglobulin by achromobacter protease I. *J. Biol. Chem.* **277** 1310–1315

Lopez De La Paz M, Goldie K, Zurdo J, Lacroix E, Dobson CM, Hoenger A and Serrano L 2002 De novo designed peptide-based amyloid fibrils. *Proc. Natl. Acad. Sci. USA* **99** 16052–16057

Losic D, Martin LL, Aguilar MI and Small DH 2006 Beta-amyloid fibril formation is promoted by step edges of highly oriented pyrolytic graphite. *Biopolymers* **84** 519–526

Morel B, Casares S and Conejero-Lara F 2006 A single mutation induces amyloid aggregation in the alpha-spectrin SH3 domain: analysis of the early stages of fibril formation. *J. Mol. Biol.* **356** 453–468

Paravastu AK, Petkova AT and Tycko R 2006 Polymorphic fibril formation by residues 10-40 of the Alzheimer's beta-amyloid peptide. *Biophys. J.* **90** 4618–4629

Petkova AT, Leapman RD, Guo Z, Yau WM, Mattson MP and Tycko R 2005 Self-propagating, molecular-level polymorphism in Alzheimer's beta-amyloid fibrils. *Science* **307** 262–265

Reches M and Gazit E 2003 Casting metal nanowires within discrete self-assembled peptide nanotubes. *Science* **300** 625–627

Reches M and Gazit E 2006 Designed aromatic homo-dipeptides: formation of ordered nanostructures and potential nanotechnological applications. *Phys. Biol.* **3** S10–19

Reches M, Porat Y and Gazit E 2002 Amyloid fibril formation by pentapeptide and tetrapeptide fragments of human calcitonin. *J. Biol. Chem.* **277** 35475–35480

Surewicz WK, Mantsch HH and Chapman D 1993 Determination of protein secondary structure by Fourier transform infrared spectroscopy: a critical assessment. *Biochemistry* **32** 389–394

Tenidis K, Waldner M, Bernhagen J, Fischle W, Bergmann M, Weber M, Merkle ML, Voelter W, *et al.* 2000 Identification of a penta- and hexapeptide of islet amyloid polypeptide (IAPP) with amyloidogenic and cytotoxic properties. *J. Mol. Biol.* **295** 1055–1071

Thompson A, White AR, McLean C, Masters CL, Cappai R and Barrow CJ 2000 Amyloidogenicity and neurotoxicity of peptides corresponding to the helical regions of PrP(C). *J. Neurosci. Res.* **62** 293–301

Thompson MJ, Sievers SA, Karanicolas J, Ivanova MI, Baker D and Eisenberg D 2006 The 3D profile method for identifying fibril-forming segments of proteins. *Proc. Natl. Acad. Sci. USA* **103** 4074–4078

Tjernberg L, Hosia W, Bark N, Thyberg J and Johansson J 2002 Charge attraction and beta propensity are necessary for amyloid fibril formation from tetrapeptides. *J. Biol. Chem.* **277** 43243–43246

Tracz SM, Abedini A, Driscoll M and Raleigh DP 2004 Role of aromatic interactions in amyloid formation by peptides derived from human Amylin. *Biochemistry* **43** 15901–15908

Ventura S, Zurdo J, Narayanan S, Parreno M, Mangues R, Reif B, Chiti F, Giannoni E *et al.* 2004 Short amino acid stretches can mediate amyloid formation in globular proteins: the Src homology 3 (SH3) case. *Proc. Natl. Acad. Sci. USA* **101** 7258–7263

von Bergen M, Barghorn S, Biernat J, Mandelkow EM and Mandelkow E 2005 Tau aggregation is driven by a transition from random coil to beta sheet structure. *Biochim. Biophys. Acta* **1739** 158–166

von Bergen M, Barghorn S, Li L, Marx A, Biernat J, Mandelkow EM and Mandelkow E 2001 Mutations of tau protein in frontotemporal dementia promote aggregation of paired helical filaments by enhancing local beta-structure. *J. Biol. Chem.* **276** 48165–48174

von Bergen M, Friedhoff P, Biernat J, Heberle J, Mandelkow EM and Mandelkow E 2000 Assembly of tau protein into Alzheimer paired helical filaments depends on a local sequence motif ((306)VQIVYK(311)) forming beta structure. *Proc. Natl. Acad. Sci. USA* **97** 5129–5134

Waddell WJ 1956 A simple ultraviolet spectrophotometric method for the determination of protein. *J. Lab. Clin. Med.* **48** 311–314

Wolf P 1983 A critical reappraisal of Waddell's technique for ultraviolet spectrophotometric protein estimation. *Anal Biochem.* **129** 145–155

Yamaguchi K, Takahashi S, Kawai T, Naiki H and Goto Y 2005 Seeding-dependent propagation and maturation of amyloid fibril conformation. *J. Mol. Biol.* **352** 952–960

Zhu M, Souillac PO, Ionescu-Zanetti C, Carter SA and Fink AL 2002 Surface-catalyzed amyloid fibril formation. *J. Biol. Chem.* **277** 50914–50922

MS received 11 October 2010; accepted 31 May 2011
*e*Publication: 00 August 2011
Corresponding editor: MARÍA ELIANO LANIO

Legends to figures

Figure 1. AFM imaging of D-ac samples obtained after incubating at pH 6 (**A** and **B**), pH 6 + mica (**C**), and pH 5 + 100 mM NaCl (**D**). Panel **B** is the 'zoomed in' region from panel **A**. Arrows indicate the fibrillar structures and are described in the text. Scale bars represent 1 µm.
Figure 2. AFM imaging of D-am sample incubated at pH 5. Scale bar represents 1 µm.
Figure 3. AFM imaging of D-am samples incubated at pH 5 in the presence of mica. The panels represent independent samples. Arrows are described in the text. Scale bars represent 1 µm.
Figure 4. AFM imaging of D-am samples incubated at pH 5 in the presence of mica and 100 mM NaCl. The panels represent images recorded for four independently prepared samples. Scale bars represent 1 µm.
Figure 5. AFM imaging of D-am samples incubated at pH 6. The panels represent images recorded from independent samples. Scale bars represent 1 µm.
Figure 6. AFM imaging of D-am samples incubated at pH 6 in the presence of mica (**A**) and in the presence of 100 mM NaCl (**B**). Scale bars represent 1 µm.
Figure 7. ATR-FTIR spectra of Amide I region of D-am (**A**) and D-ac (**B**) after drying the peptides (4 nmol) from water.
Figure 8. Far-UV CD spectra of D-am at pH 5 (**A**) and pH 6 (B) without (**▬**) and with (—) 100 mM NaCl. Spectra of D-ac at pH 5 (**C**) and pH 6 (**D**) without (**▬**) and with (—) 100 mM NaCl.

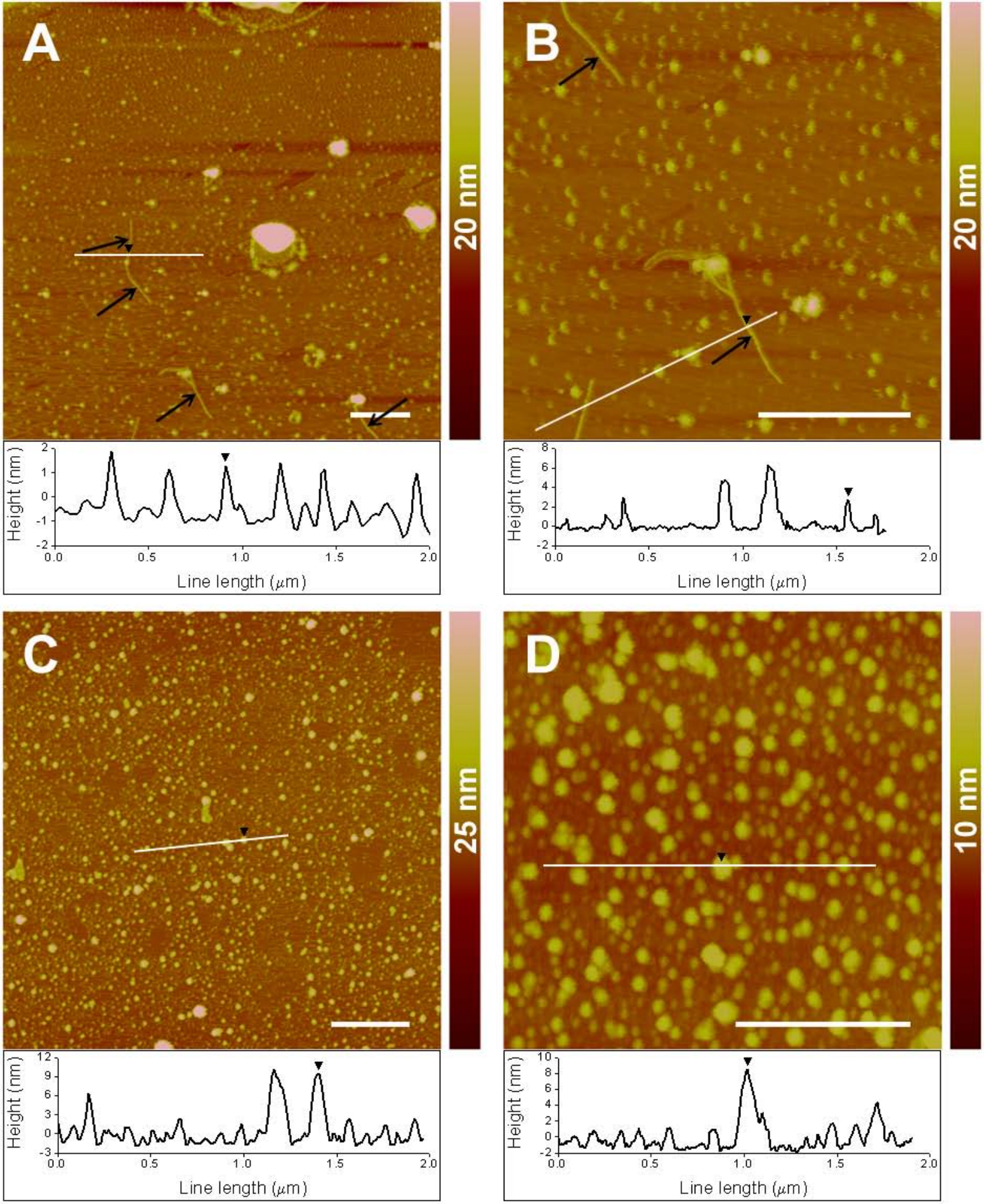
A
20 nm
Height (nm)
Line length (μm)
B
20 nm
Height (nm)
Line length (μm)
C
25 nm
Height (nm)
Line length (μm)
D
10 nm
Height (nm)
Line length (μm)

Figure 1

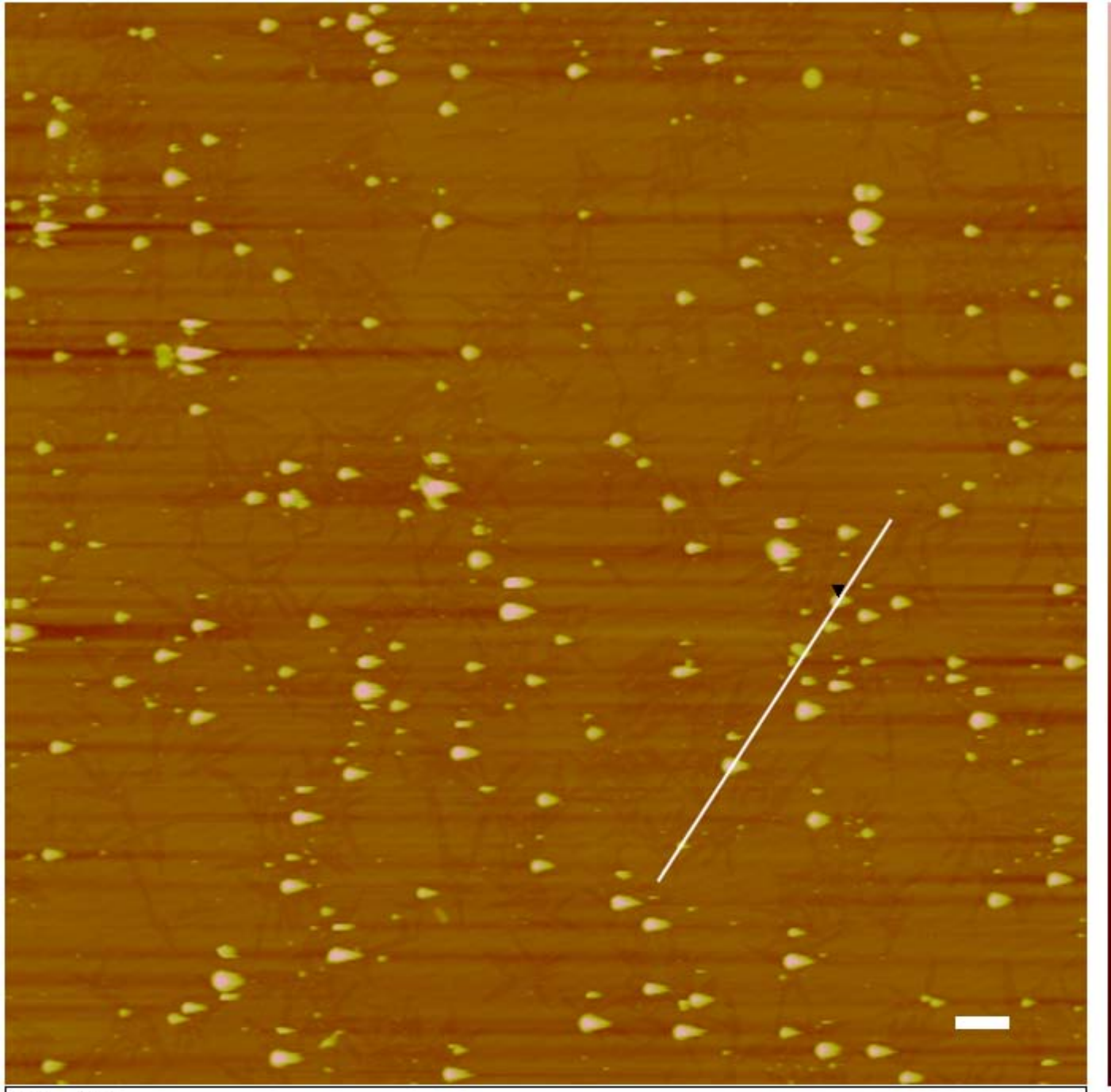

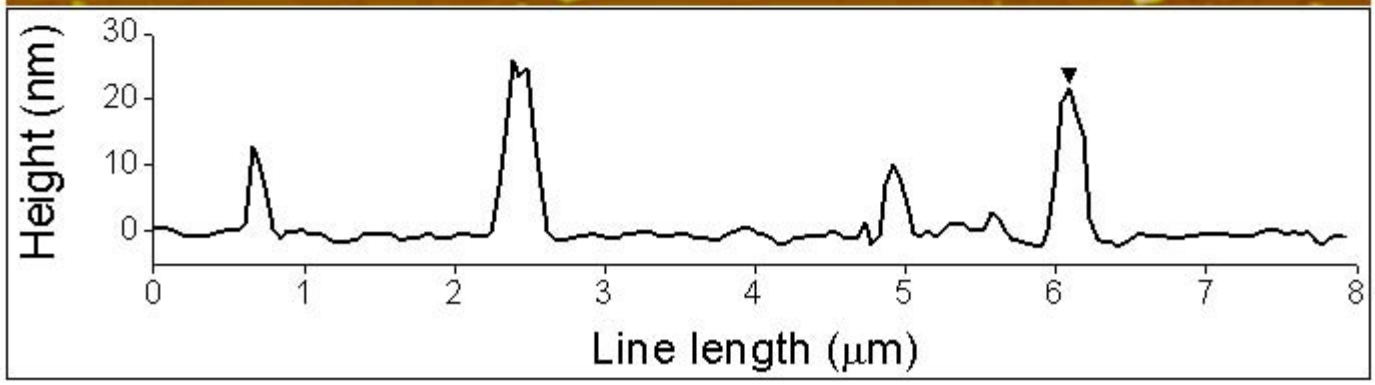

Figure 2

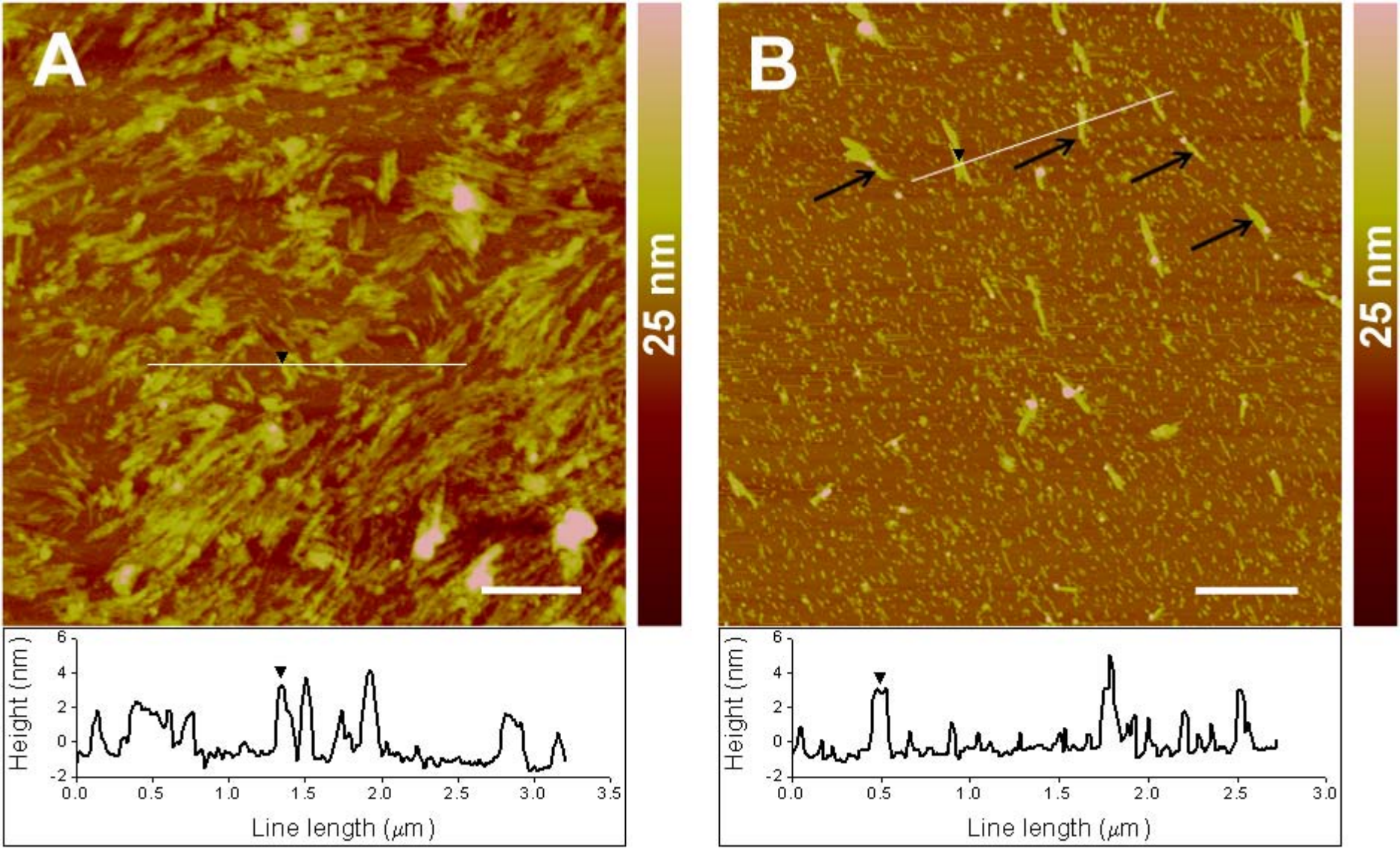
A
25 nm
Height (nm)
6
4
2
0
-2
0.0
0.5
1.0
1.5
2.0
2.5
3.0
3.5
Line length (μm)
B
25 nm
Height (nm)
6
4
2
0
-2
0.0
0.5
1.0
1.5
2.0
2.5
3.0
Line length (μm)

Figure 3

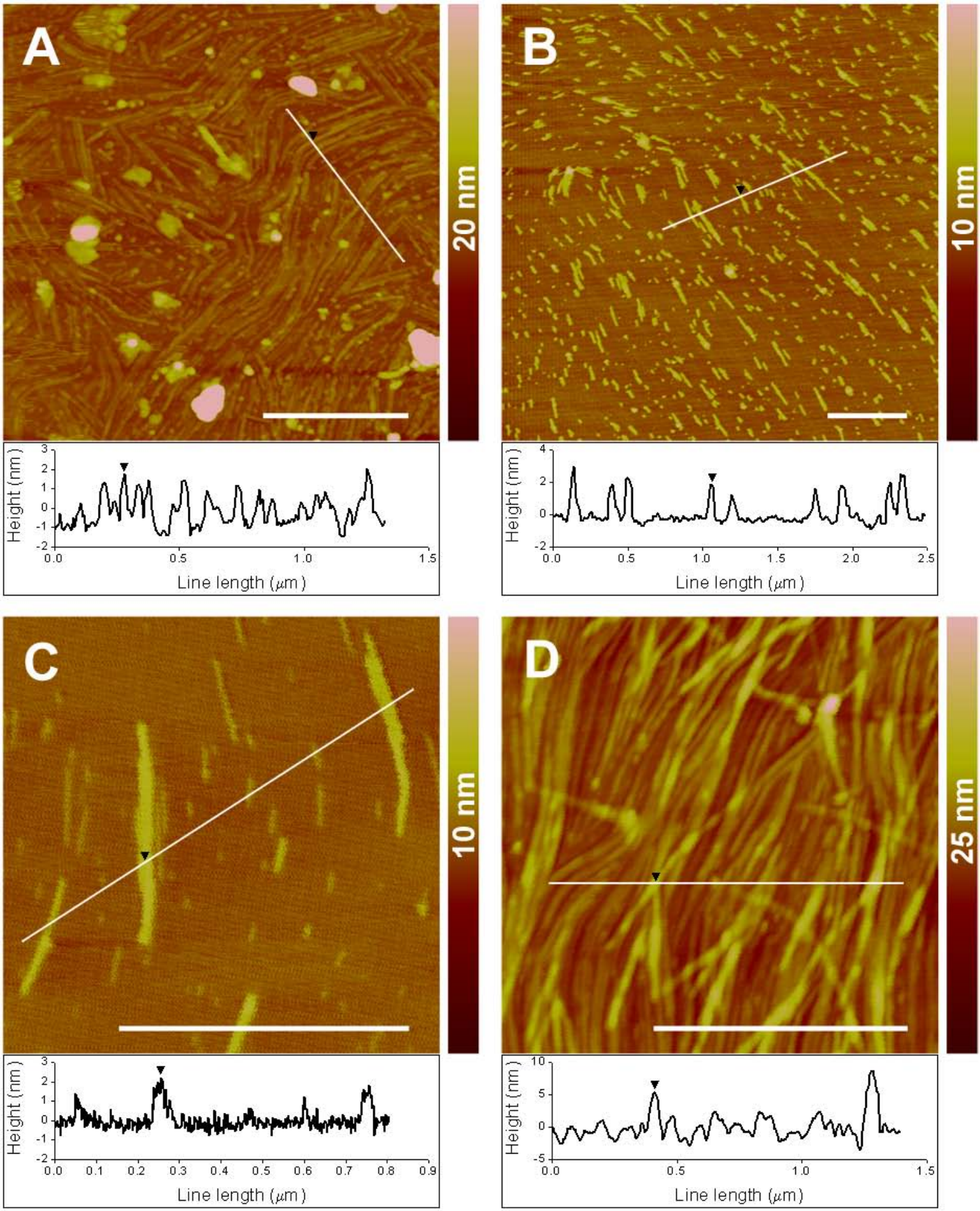
A
20 nm
Height (nm)
3
2
1
0
-1
-2
0.0
0.5
1.0
1.5
Line length (μm)
B
10 nm
Height (nm)
4
2
0
-2
0.0
0.5
1.0
1.5
2.0
2.5
Line length (μm)
C
10 nm
Height (nm)
3
2
1
0
-1
-2
0.0
0.1
0.2
0.3
0.4
0.5
0.6
0.7
0.8
0.9
Line length (μm)
D
25 nm
Height (nm)
10
5
0
-5
0.0
0.5
1.0
1.5
Line length (μm)

Figure 4

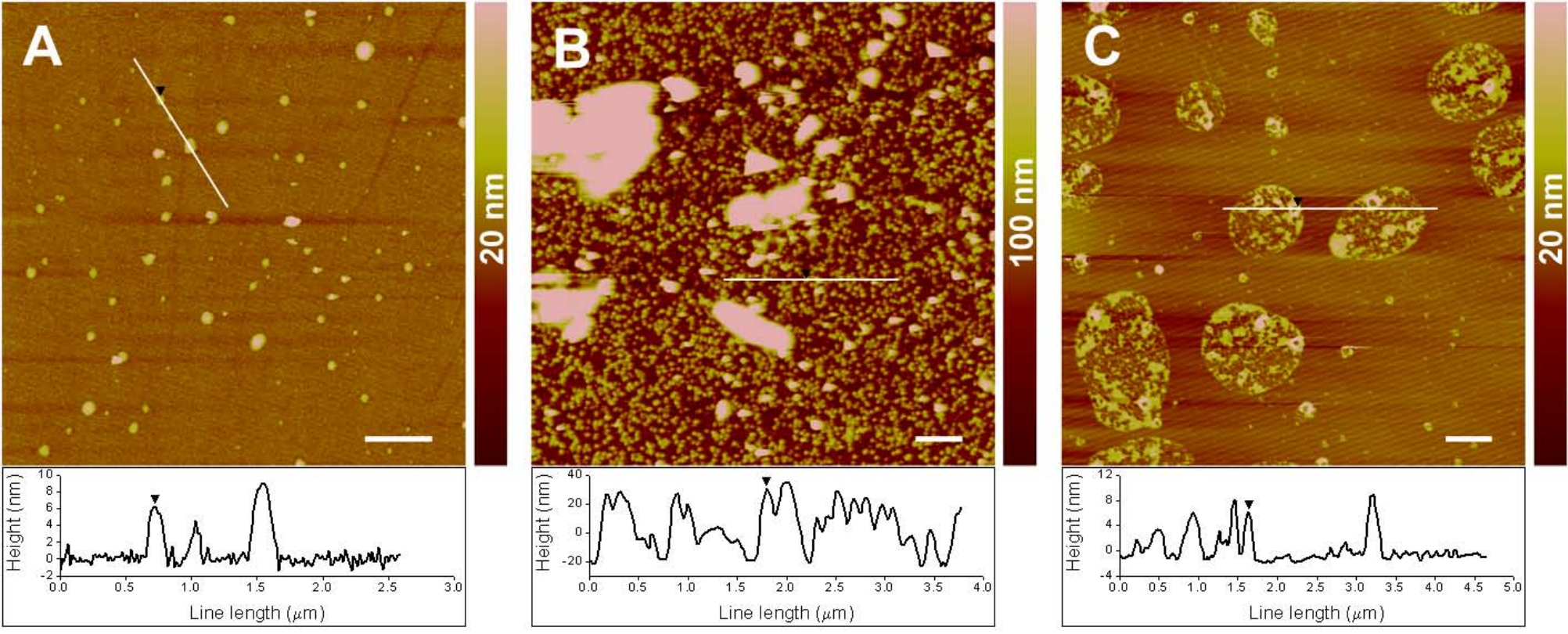
A
20 nm
Height (nm)
10
8
6
4
2
0
-2
0.0
0.5
1.0
1.5
2.0
2.5
3.0
Line length (μm)
B
100 nm
Height (nm)
40
20
0
-20
0.0
0.5
1.0
1.5
2.0
2.5
3.0
3.5
4.0
Line length (μm)
C
20 nm
Height (nm)
12
8
4
0
-4
0.0
0.5
1.0
1.5
2.0
2.5
3.0
3.5
4.0
4.5
5.0
Line length (μm)

Figure 5

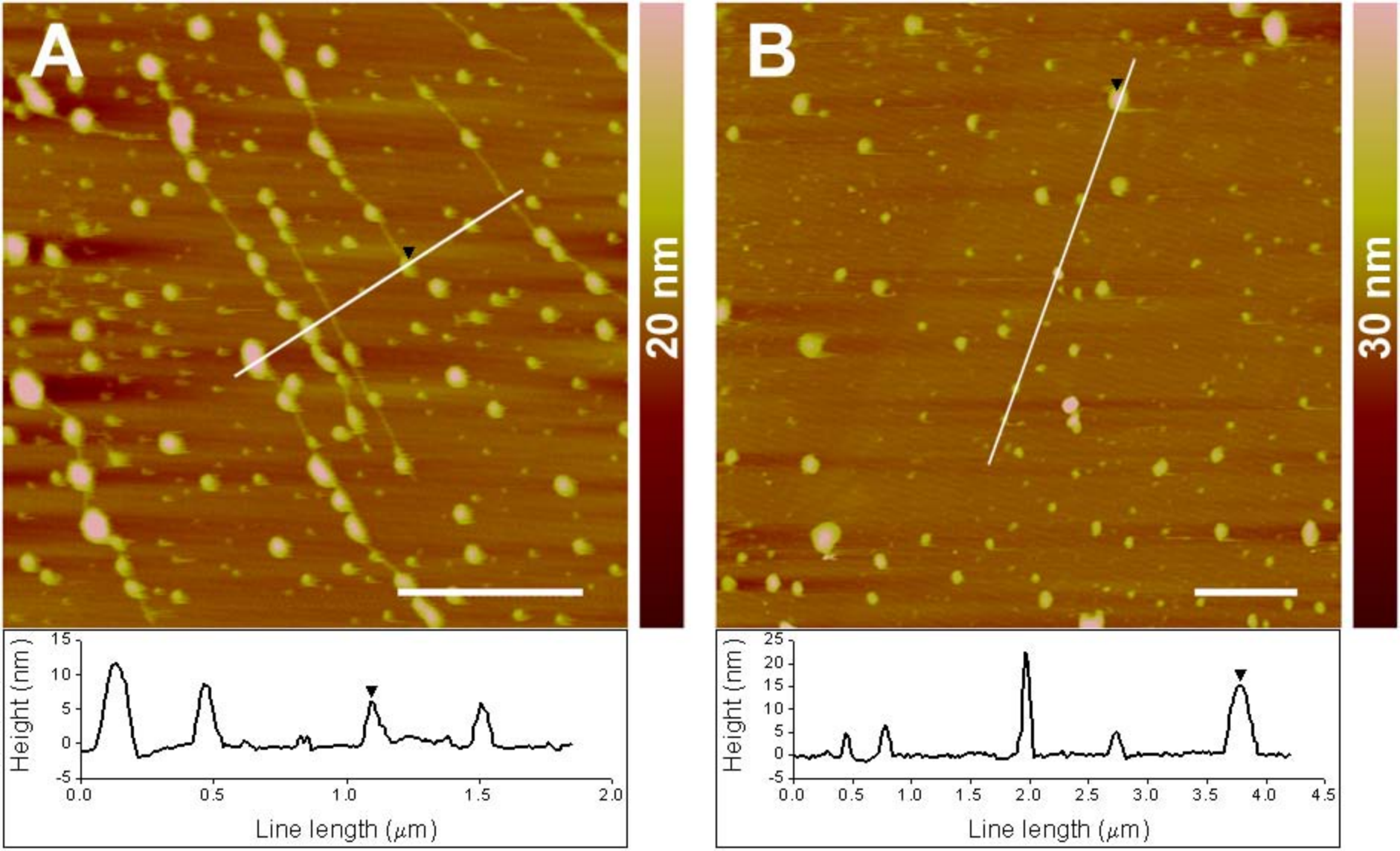
A
20 nm
B
30 nm
Height (nm)
Line length (μm)
Height (nm)
Line length (μm)

Figure 6

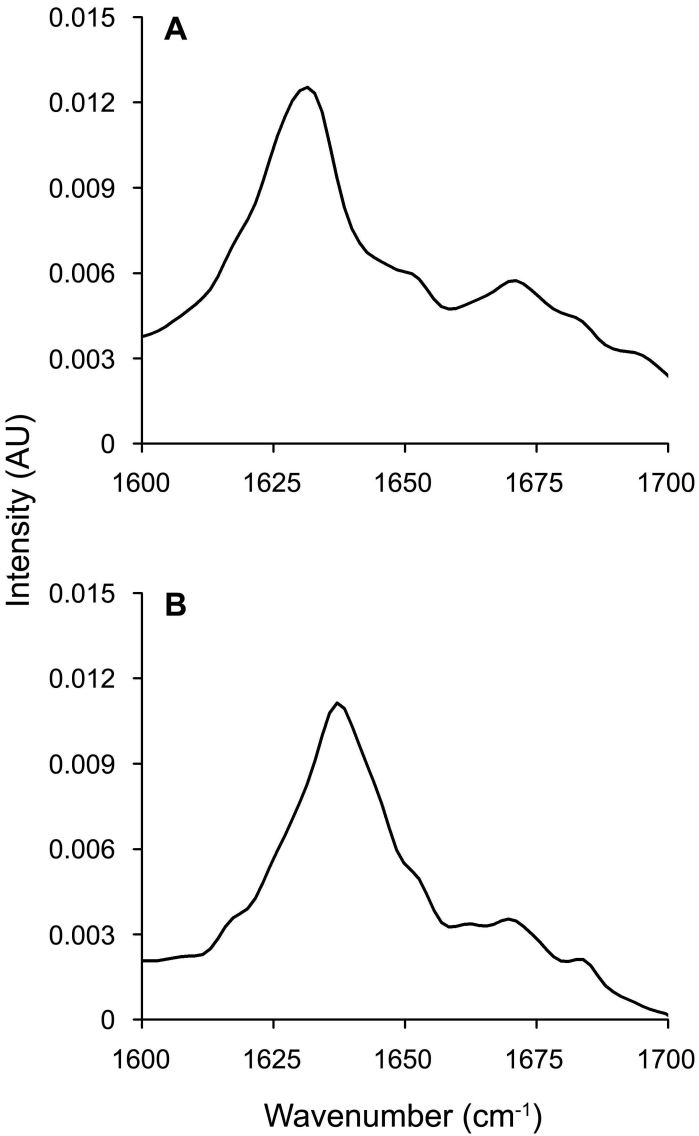
A
B
0.015
0.012
0.009
0.006
0.003
0
1600
1625
1650
1675
1700
Intensity (AU)
Wavenumber (cm-1)

Figure 7

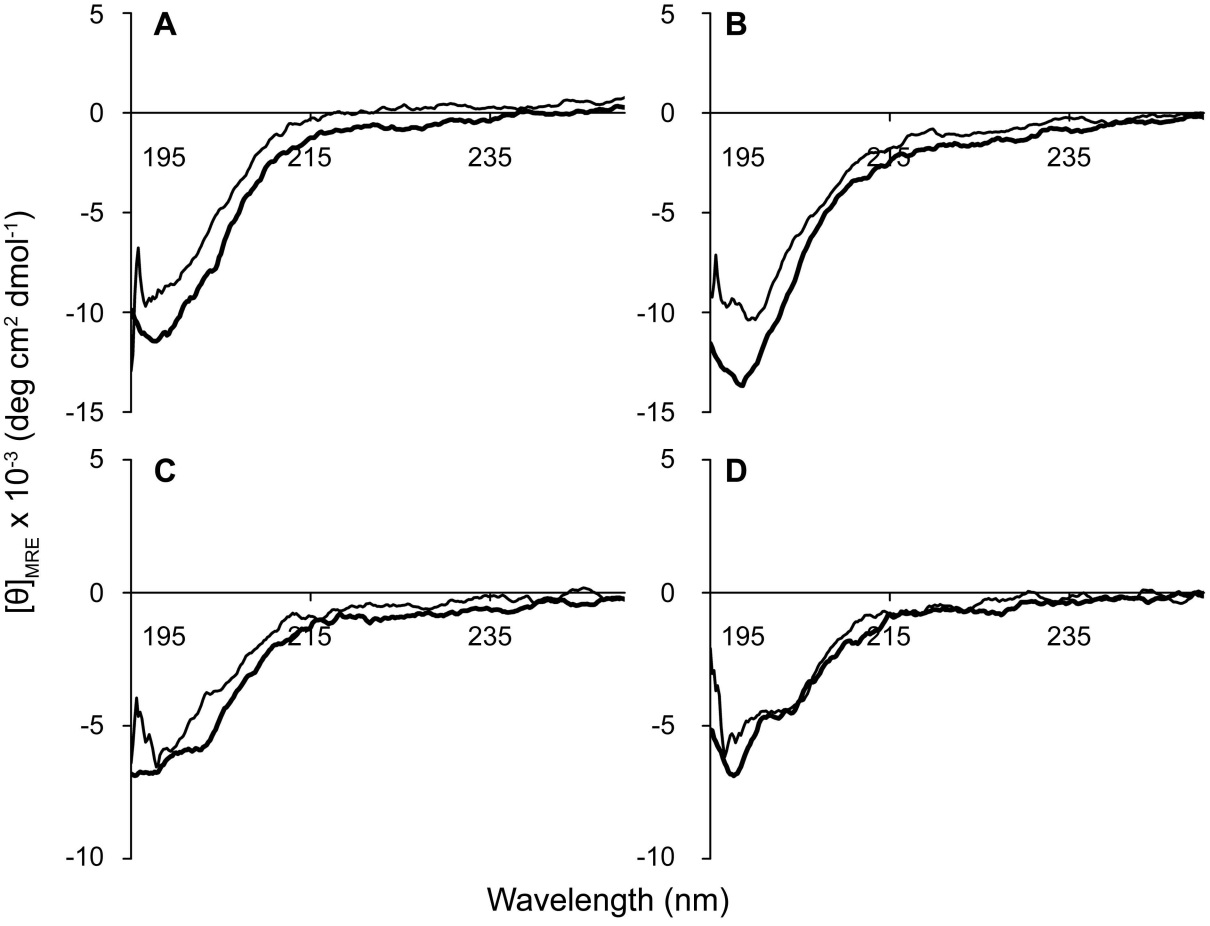
A
B
C
D
5
0
-5
-10
-15
195
215
235
$[\theta]_{MRE}$ x 10^{-3} (deg cm^2 $dmol^{-1}$)
Wavelength (nm)

Figure 8